Molecular Dynamics-Assisted Interaction of Vanadium Complex-AMPK: from the force field development to biological application for Alzheimer's treatment

Camila A. Tavares[1], Taináh M. R. Santos[1], Elaine F. F. da Cunha[1] and Teodorico C. Ramalho[1,2*]

[1] Laboratory of Molecular Modelling, Department of Chemistry, Federal University of Lavras, Lavras – MG, 37200-000, Brazil.

[2] Department of Chemistry, Faculty of Science, University of Hradec Králové, Hradec Králové, 500 03, Czech Republic.

[*] **Corresponding Author:**

Teodorico de Castro Ramalho

e-mail: teo@ufla.br

Abstract

Large part of the world population is affected by Alzheimer's disease (AD) and diabetes mellitus type 2, which causes both social and economic impacts. These two conditions are associated to one protein, AMPK. Studies have shown that vanadium complexes, such as bis(N',N'-dimethylbiguanidato)-oxovanadium (IV), $VO(metf)_2 \cdot H_2O$, are potential agents against AD. A crucial step on drug design studies is obtaining information about the structure and interaction of these complexes with the biological targets involved in the process through Molecular Dynamics (MD) simulations. However, MDs depend on the choice of a good force field that could present reliable results. Moreover, general force fields are not efficient for describing the properties of metal complexes, and a $VO(metf)_2 \cdot H_2O$-specific force field does not yet exist, thus the proper development of a parameter set is necessary. Furthermore, this investigation is essential and relevant given the importance for both the scientific community and the population that is affected by this neurodegenerative disease. Therefore, the present work aims to develop and validate the AMBER force field parameters for $VO(metf)_2 \cdot H_2O$, since the literature lacks such information on metal complexes, and investigate through classical molecular dynamics the interactions made by the complex with the protein. The proposed force field proved to be effective for describing the vanadium complex (VC), supported by different analysis and validation. Moreover, it had a great performance when compared to general AMBER force field. Beyond that, MD findings provided an in-depth perspective about vanadium complex-protein interactions that should be taken into consideration in future studies.

Keywords: Vanadium Complex. AMBER Force Field. Molecular Dynamics. Docking. Alzheimer’s Disease.

1. Introduction

According to data published by World Health Organization (WHO) and United Nations (UN), life expectancy has increased in the last 20 years, reaching 72.28 years, worldwide.[1,2] Furthermore, records show that between years 1950 and 2020, life expectancy increased 25.3 years. Regarding elderly people, it increased, in average, 6.7 years during the same period.[1] However, such milestone is not achieved due to a reduction of years lived with disability but because of a decrease of mortality. In other words, the increasing on life expectancy does not necessarily improve the quality of life of a population. The health of the population plays an important role on such statistic indicator.[1]

One of the conditions that most affects health and is most prevalent among the elderly population is dementia. Based on data reported by WHO, it affects around 50 million people worldwide. Dementia is a general term for neurodegenerative diseases, with Alzheimer's Disease (AD) being the most commonly known, occurring in about 60-70 % of dementia cases.[2]

AD is a neurodegenerative disorder that is known for loss of cognitive functions and memory. Its symptoms may include difficulties on solving problems, completing ordinary tasks, and keeping track of time, in addition to the inability to retrieve the name of relatives, mood swings and withdrawal from social interaction. It affects elderly people in its majority, and it is related to aging of the cells from the nervous system. The aging process of the nervous system, in turn, is related to the programmed cell death, also known as apoptosis, triggered by beta-amyloid peptide.[3]

Due to its complexity, the etiology of AD is still uncertain. However, some hypotheses have been proposed regarding the factors that may influence on its development.[4,5] Despite directly targeting one of the most acceptable hypotheses to seems a safe approach,[6] it is known that some obstacles have not yet been overcome, leading to a failure in the search for agents associated with the therapy of this disease[7] or even, the discovery of new treatments may require novel approaches, which is quite challenging.[8]

One of them associates the development of AD to type 2 diabetes mellitus (T2DM) in which the link between those two conditions is the protein kinase AMPK, where the progression of T2DM can lead to cognitive impairment.[9] Furthermore, there is a possibility that T2DM may affect the development of AD through the insulin signaling in the brain.[10]

5' AMP-activated protein kinase (AMPK) is a metabolic enzyme that plays important roles in both AD and T2DM.[9] Studies have shown that such enzyme can increase the glucose transport and regulate free fatty acids, in T2DM.[11] Moreover, in AD, AMPK can reduce Aβ expression and indirectly inhibit hyperphosphorylation of tau.[12] In this sense, AMPK may be an excellent biological target in studies where the prevention and treatment of AD are the main goal.

Some treatments are available in order to reduce the cognitive impairment even though the cure has not been discovered yet.[13] Approaches include targeting different pathways, for instance, exploring the possibility of the use of drugs that are already used in the treatment of T2DM as possible candidates for AD treatment.[14] Different metal complexes have been investigated based on their potential application in AD. Among those complexes are platinum, ruthenium, iridium, rhodium, cobalt, and vanadium complexes.[15]

A great example of a vanadium complex (VC) that has shown to be efficient in the treatment of T2DM and is considered a potential agent against AD is bis(N',N'-dimethylbiguanidato)-oxovanadium (IV), $VO(metf)_2 \cdot H_2O$ (Figure 1). Studies have indicated the good performance of $VO(metf)_2 \cdot H_2O$ in decreasing the level of insulin in rats, in other words, this VC led to a more promising antidiabetic response than its ligand metformin, known to be an efficient antidiabetic.[16] Furthermore, it has also been shown that such VC had its action compared to BMOV, a reference in the treatment of diabetes, where its efficiency was quite similar to the compound in question.[17] Thus, vanadium complexes, specially $VO(metf)_2 \cdot H_2O$, deserve all attention from the scientific community due to their potential effect against diseases.

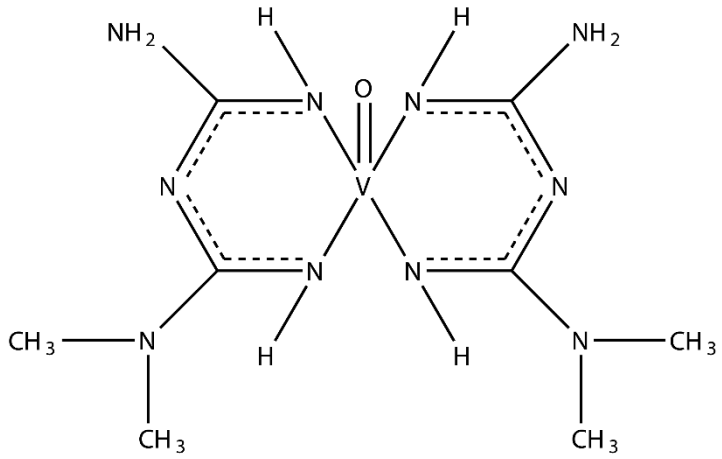

Figure 1. Structure of bis(N',N'-dimethylbiguanidato)-oxovanadium (IV), VO(metf)$_2$·H2O.

To provide relevant and valuable information about interactions of such complexes in the biological environment, computational investigations may be of significant benefit.[18] Classical Molecular Dynamics (MD) is one of the mostly used tools to assist in further drug design studies.[19] MD relies on a proper choice of force fields (FF) to describe systems, and regarding inorganic compounds, information such as parameters to describe the molecules are somewhat scarce and need to be developed.[20,21] Furthermore, general force fields may not accurately describe the molecule,[22] reinforcing the idea that developing a new force field for metal-centered molecules is essential. Interestingly, force fields for VO(metf)$_2$·H$_2$O are yet to be described in the literature and will be approached in this work.

In the light of the foregoing, this work aims to obtain the AMBER force field parameters of the VO(metf)$_2$·H$_2$O, due to its potential action against AD. Thus, it is believed that the work may contribute to further parameterization studies of metal complex force field, enabling the investigation of compounds with potential effect for the treatment of AD. To accomplish this, the first step was to develop the force field for the vanadium complex. Then, an MD simulation in vacuum was performed in order to investigate the structural behavior of such complex and this new force field was validated by comparing with the data derived from DFT calculations. After that, the docking study with VO(metf)$_2$·H$_2$O and the protein AMPK was performed, where the best lower energy pose that reproduced interactions already described by the literature was selected as a starting point for the study of the behavior of the system through MD simulation.

2. Computational Details

Structural Optimization

The initial structure of the vanadium complex under study was built using the software GaussView 5.0.8.[23] A relaxed potential energy surface (PES) scan of the two

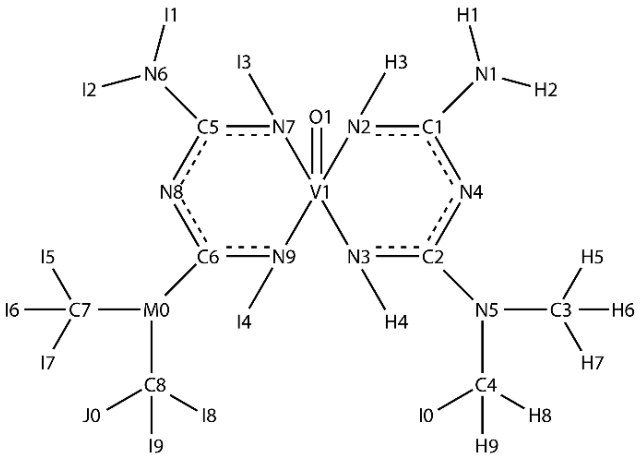

Figure 2. Atom types assigned to the VC. N and M, C, H and I, O, and V represent nitrogen, carbon, hydrogen, oxygen, and vanadium atoms respectively.

dihedrals (N8-C6-M0-C8 and N4-C2-N5-C4) (Figure 2) were conducted. Such conformational analysis was performed through DFT calculations, using B97-D functional and 6-311G++ basis function.[24] Since it is highly important to have a reference with a global minimum energy, and consequently, aiming for a system with an accurate structure, the optimization of the molecule with theory level B3LYP and basis set def2-TZVP plus LANL2DZ ECP for vanadium atom was obtained using Gaussian 09[25] as a starting point for the development of the force field. Evidence showed that hybrid B3LYP exchange correlation functional in combination with polarized valence triple-zeta basis set were adequate to describe a system containing vanadium, presenting results with good agreement when comparing to experimental data.[26] In addition, an optimization through Molecular Mechanics method, using the AMBER force field was found through the software HyperChem 7.0[27] for further investigation and comparison.

Although the metal atom present in the complex is relatively lighter than other metals and does not present prominent relativistic effects, a calculation using the software ORCA 4.0[28] was performed, adopting the B3LYP functional and def2-TZVP as a basis 4set with relativistic method ZORA.[29] Such investigation was carried out to analyze if the results provided by the quantum mechanical (QM) calculation (LANL2DZ ECP) are close to the ones provided by the relativistic ZORA method.

Development of the New Amber force field

To better describe the system under study and develop a set of parameters, an identification and labeling of the structure were performed. Although automatic tools are used to model systems of interest,[30] it is crucial to guarantee that the molecule to be described represents a structure as close to reality as possible. Using atom types in this set of parameters allows to distinguish the atoms in a better manner, considering structural and vibrational characteristics.[21]

Using the VMD 1.9.1 software,[31] the atom types were assigned utilizing two characters (one letter and one number) due to AMBER simulation package requirement, where C represent carbon atoms; N and M, nitrogen atoms; H and I, hydrogen atoms, O, oxygen atoms and V, vanadium atom, as shown Figure 2.

The parameterization was carried out adopting the structure with global minimum energy derived from the DFT calculations. Thus, the potential energy (V_{total}) of a molecule can be described as a summation of all terms that are involved in the system total energy, i.e., the total potential energy equals to the sum of bonded terms (bond, angles, and dihedrals) and non-bonded terms (Coulomb and Lennard-Jones), as stated by Equation 1:

$$V_{total} = \sum_{bonds} K_b(b - b_0)^2 + \sum_{angles} K_\theta(\theta - \theta_0)^2 + \sum_{dihedrals} K_\phi\,[cos(n\phi\ -\ \delta) + 1]$$

$$+ \sum_{Coulomb} \left[\frac{q_i q_j}{4\pi\varepsilon_0 r_{ij}}\right] + \sum_{Lennard-Jones} 4\epsilon_{ij}\left[\frac{\sigma^{12}}{r_{ij}^{12}} - \frac{\sigma^6}{r_{ij}^6}\right] \qquad (1)$$

where K_b, K_θ, and K_Φ are the force constants, b and θ correspond to bond length and angle respectively, b_0 and θ_0 are the equilibrium values, n is the periodicity, ϕ represents the dihedral angle, δ is the phase angle, r_{ij} is the distance between atoms i and j, ϵ is the depth of the potential well, σ is the distance at which the Lennard-Jones Potential is zero, q_i and q_j are the partial atomic charges of each atom, and ε_0 corresponds to vacuum permittivity.[32]

Further, from Equation 1, it can be seen that the AMBER force field is able to approximate the energy surface based on Newton's equations of motion, describing the forces acting on each atom due to the contributions of bonded and non-bonded atoms,

emphasizing one of the two assumptions involved in common force fields, additivity, i.e., the overall energy associated to a system is the sum of different potentials with simple physical interpretations.[33] It is important to highlight that in this case, proper dihedrals were considered sufficient to describe the structure of CV, thus parameters for the improper dihedrals are absent.

The Hessian matrix calculation from the global minimum geometry was performed using the same functional and basis set as stated earlier in this chapter (B3LYP/def2-TZVP plus ECP for the vanadium atom). Based on the internal coordinate method, the force constants for the bonded terms were acquired through diagonalization of the Hessian matrix. It is noteworthy mentioning that since the obtained parameters highly depend on the internal coordinates originated from the QM calculation, different internal coordinates will result in different force constants.[34] The calculation of the Restrained Electrostatic Potential (RESP) atomic charges was carried out to obtain the Coulomb interaction parameters. Lastly, the Lennard-Jones parameters for all atoms, except vanadium, were assigned based on General AMBER Force Field (GAFF) values. The non-bonded Lennard-Jones parameters ϵ and σ for vanadium atom were attributed according to values found in the literature.[35]

Once all the information needed about the parameters of VC was acquired, an MD simulation in vacuum was performed, at room temperature (T=300 K) and total simulation time of 20 ns, using AMBER11 simulation package.[36] Finally, a comparison between the structural data set and a quantum reference was made, considering only the last 10 ns of the simulation to ensure that the equilibration of the molecule was reached.

Docking Studies

The 3D structure of the protein AMPK was obtained from RCSB Protein Data Bank (PDB ID: 6C9G).[37] Due to absence of some residues of amino acids and aiming a more realistic structure to avoid inaccurate representations, a preparation of the protein was conducted. For this, the platform SWISS-Model was used to generate a homology model of the 3D structure based on templates available on the server.[38] After that, an alignment of the model obtained by the last step was performed through LovoAlign server.[39] The list of the equivalence of the residues in the original PDB file and the homology model generated by this step can be found in Table S1.1 in the Support Information (SI).

BIOVIA Discovery Studio Visualizer v. 21[40] was used to prepare the protein structure, where hydrogens atoms were added, and charges were calculated. Molegro Virtual Docker 2011 was used for the docking studies.[41] Based on the information reported by literature,[42] the antidiabetic drug known as metformin interacts with residues from AMPK-α1, namely Asp-217, Asp-218, and Asp-219. Such residues are equivalent to residues Asp-215, Asp-216, and Asp-217 in the homology model. Considering that the vanadium complex under study has two metformin as ligands, the previous information was considered to be a great insight about the docking site. Regarding the parameters used for the investigation, the flexible residues were included within a radius of 8 Å and the binding site radius was set as 7 Å. The score algorithm used was MolDock Score [GRID] with grid resolution of 0.30 Å and the search algorithm used was MolDock Optmizer.[43]

Molecular dynamics simulation

Simulations were conducted using the AMBER20 package and Amber ff99SB-ILDN force field[44] for the protein and were divided in four steps, namely minimization, heating, equilibration and production. The first step was performed by minimizing the energy of the system with 2000 cycles of steepest descent method with a system restriction of 500.0 kcal/mol followed by 8000 cycles of conjugate gradient method. Next, the temperature of the system was increased gradually from 0 to 300 K in 5 steps of 50 ps each using the NVT ensemble and equilibrated at the same temperature, where the restriction was systematically decreased. Finally, for the production step, the simulation was performed with explicit solvent, using the TIP3P model, during 800 ns, without any restraint and in the presence of counterions, to maintain the neutrality of the simulated systems.[44] The final system included the AMPK protein, around 84,853 water molecules, and one Cl^- ion, leading to a simulated system that contains 270,496 atoms.

3. Results and Discussion

Conformational Search and Structural analysis

$VO(metf)_2 \cdot H_2O$ was previously optimized through Molecular Mechanics to avoid possible convergence errors, where UFF (Universe force field) was used for this calculation. The optimization was carried out using the Gaussian software. Then, the molecule in question was subjected to the scan calculation, in which the dihedrals N8-

C6-M0-C8 and N4-C2-N5-C4 had their torsion angles varied, with increments of 30°. For this DFT calculation, B97-D functional and 6-311G++ basis function was used. As a result, the conformation with energy of -1,181,845.70 kcal/mol was chosen as the most stable and the one that better described the structural properties of the vanadium complex in a more realistic way.

Next, DFT calculations from different software, B3LYP/def2-TZVP LANL2DZ ECP (Gaussian) and B3LYP/def2-TZVP ZORA (ORCA) were performed, besides the optimization of the molecule using AMBER force field available on HyperChem. The results obtained by forementioned step were compared in order to evaluate the performance of the level of theory chosen to describe the system in question.

The structural validation included a total of 41 bonds and 72 bond angles and will be promptly addressed. The obtained results are available in Tables 1 and 2, where selected bond lengths and angles are shown in angstroms and degrees, respectively. The full information is available in SI (Tables S2.1 and S2.3).

Table 1. Selected bond lengths in Angstroms (Å) of different methods and levels of theory.

	AMBER *(HyperChem)*	**B3LYP/def2-TVZP LANL2DZ ECP** *(Gaussian 09)*	**B3LYP/def2-TVZP ZORA** *(ORCA)*
N2-V1	1.839	2.037	2.042
N3-V1	1.843	2.055	2.051
V1-O1	1.880	1.579	1.595
N7-V1	1.848	2.046	2.043
N9-V1	1.846	2.045	2.050

According to the gathered information, optimization using AMBER force field available on HyperChem did not present results with good agreement when compared with data obtained by a quite robust method (B3LYP/def2-TZVP ZORA), which re-emphasizes the need for more accurate AMBER force field parameters to describe the system under discussion.

Table 2. Selected bond angles in degrees (°) of different methods and levels of theory.

	AMBER *(HyperChem)*	**B3LYP/def2-TVZP LANL2DZ ECP** *(Gaussian 09)*	**B3LYP/def2-TVZP ZORA** *(ORCA)*
N2-V1-O1	117.754	110.114	108.146
N3-V1-O1	115.619	106.161	107.364
N2-V1-N7	80.736	87.063	86.898
N3-V1-N9	77.617	86.725	87.060
N3-V1-N7	130.033	147.690	144.919
N2-V1-N9	128.385	139.820	144.056
N2-V1-N3	84.467	82.159	82.377
V1-N3-C2	123.096	130.690	130.317
C5-N7-V1	118.600	128.866	128.800

It is possible to notice that the AMBER force field available on HyperChem fails to describe the structure of the complex when compared to relativistic method ZORA in which the mean of relative error for bond lengths and bond angles do not present reliable values. Such information can be retrieved in Table S2.5, in the SI.

The comparison between the relativistic method ZORA and the DFT calculation performed on Gaussian was carried out in order to investigate whether the minimized geometry obtained with ECP would present a geometry close to the one provided by the relativistic ZORA method, since no experimental data for the vanadium complex was available.

From Tables 1 and 2, it is possible to evaluate the calculations performed in Gaussian and ORCA, suggesting that the B3LYP/def2-TVZP LANL2DZ ECP level of theory used in this work to obtain the lowest energy geometry of the vanadium complex is as effective as the relativistic ZORA method. It is relevant to point out that when considering the effective core potential (ECP), any substantial increase in computational cost was not experienced. Moreover, the level of theory chosen for the optimization of the VC under study showed good performance on describing the structure of the system.

Validation of the New Force Field

In this step of validation, a comparison of bond lengths and bond angles was made among the values obtained from the quantum reference and the simulations using the new

force field and GAFF, being possible to assess the deviations that the force field under study has in contrast with the reference and the general AMBER force field available on HyperChem. Furthermore, this investigation was performed considering the last 10 ns of the MD simulations.

According to Table 3, a good agreement between the values of bond lengths of the new force field and values derived from the DFT calculation was found. The complete comparison, including all bonds, can be found in SI, Table S3.1. It is noticeable that the new force field had a better performance regarding describing the bonds of the system under study. The mean of relative error (Table S3.5) obtained by the force field developed in this work showed smaller value (0.671%) when compared to the mean of relative error from GAFF (1.345%), which suggests that the general force field could not describe the bonds as efficient as the new force field.

Table 3. Selected bond lengths in Angstroms (Å) obtained by different calculations for validation purposes.

	B3LYP/def2-TVZP+LANL2DZ ECP *(Gaussian 09)*	**MD with GAFF** *(average)*	**MD with New FF** *(average)*
N2-V1	2.037	2.012	2.046
N3-V1	2.055	2.072	2.037
V1-O1	1.579	1.569	1.570
N7-V1	2.046	1.999	2.050
N9-V1	2.045	2.050	2.037

The good results obtained by the new force field is more pronounced when analyzing the bond angles, where the same pattern can be observed (Table 4). The new force field showed values closer to the reference (5.407%), with smaller mean of relative error (Table S3.5) when comparing to the values obtained by the GAFF simulation (7.345%). Once again, the new parameter set showed better performance than the general and widely used GAFF.

Table 4. Comparison of selected bond angles (º) obtained by different calculations for validation purposes.

	B3LYP/def2-TVZP+LANL2DZ ECP *(Gaussian 09)*	**MD with GAFF** *(average)*	**MD with New FF** *(average)*
N2-V1-O1	110.114	113.600	106.256
N3-V1-O1	106.161	48.671	98.213
N2-V1-N7	87.063	47.201	60.949
N3-V1-N9	86.725	53.313	128.946
N3-V1-N7	147.690	73.493	127.501
N2-V1-N9	139.820	100.064	130.776
N2-V1-N3	82.159	66.947	74.303
V1-N3-C2	130.690	131.880	131.775
C5-N7-V1	128.866	124.994	126.351

The results obtained by this analysis reinforce the importance of developing parameters for $VO(metf)_2 \cdot H_2O$ in order to describe the structure of the system with more accuracy.

New Amber Force Field Performance

The evolution of MD simulation in vacuum was monitored by a time-dependent calculation of the root mean square deviation (RMSD). It should be noted that the structure derived from DFT calculations was taken as a reference for such analysis. It is important to mention that the total time of simulation was 20 ns, however for the analysis, only the last 10 ns were considered in order to assure that the complex reached equilibrium. Based on Figure 3, it is possible to observe that during the last 10 ns, the structure under study had an amplitude of oscillation of 0.5 Å, with average of RMSD equal to 0.839 Å ± 0.002 Å. Moreover, RMSD analysis demonstrates that the equilibrium condition was achieved, in other words, the complex attained a stable conformation. It is important to note that the simulation was carried out in vacuum, i.e., in the absence of molecules that could restrict the flexibility of the molecule.

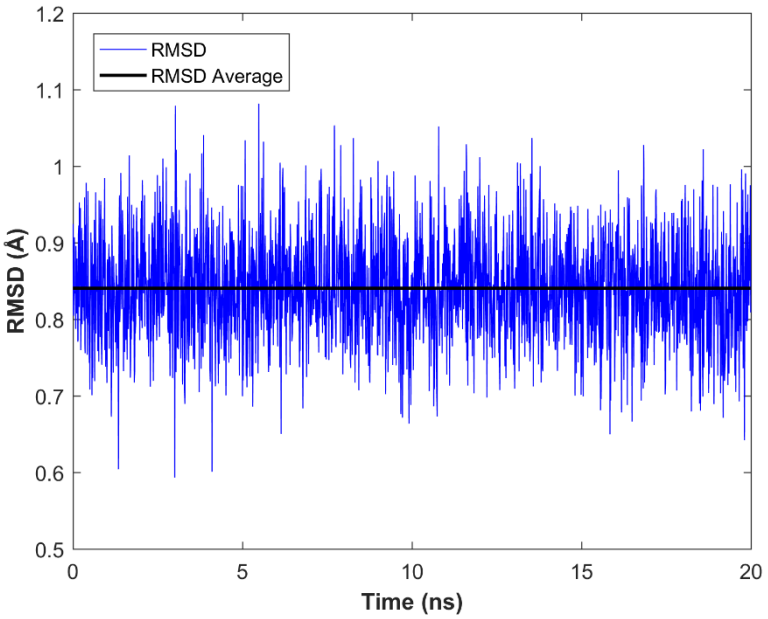

Figure 3. RMSD vs. time graph calculated for vanadium (IV) complex in vacuum.

In addition to the analysis of the VC in vacuum, an MD simulation in aqueous solution (Figure S4.2), using the TIP3P model for water molecules was carried out as well. Once again, the complex achieved a stable conformation, where the RMSD analysis shows equilibrium condition of the molecule under study. Moreover, VC presented amplitude of oscillation of 0.701 Å with average of RMSD equal to 0.337 Å ± 0.003 Å.

Bond Length Alternation

The geometric analysis of bond length alternation (BLA) was performed as well. The calculation of BLA is mathematically described by Equation 2:

$$BLA = \frac{1}{N_s}\sum l_S - \frac{1}{N_D}\sum l_D \qquad (2)$$

where N_S is the number of conjugated single bonds, N_D is the number of conjugated double bonds, l_S and l_D are the length of single and double bonds respectively.

A system is considered ideally conjugated when the average of the difference between single and double bond lengths is equal to zero. The average BLA values of the geometry were extracted from the last 10 ns of MD simulation for the new force field and

GAFF. Figure 4 shows the BLA models computed from quantum reference (0.010 Å) in addition to the MD simulation using the new force field (0.009 Å) and GAFF (0.006 Å) parameters. According to the graph, the value obtained for the new force field showed very good agreement between the DFT approach, accurately describing the complex and proving the quality of the developed parameter set.

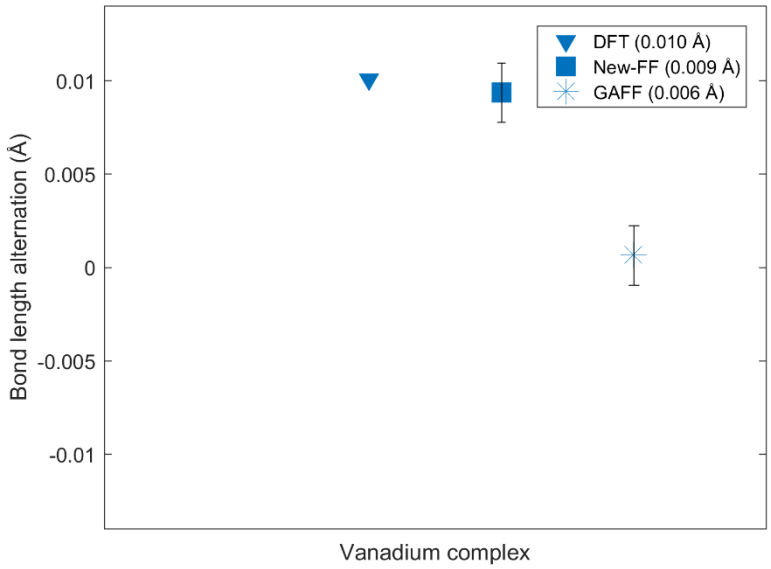

Figure 4. BLA analysis comprised of mean values of bond lengths from different models based on DFT, GAFF and New Force Field.

Protein Preparation

For the protein structure homology modelling, 123 residues were inserted to the structure whilst four residues were removed. A complete table with all residues from the model and the original structure is available in S1.1, where it is possible to see all equivalents residues. Moreover, the structure used as a template (SMTL ID: 5ezv.1) showed parameters closer to 1, i.e., parameters considered to be more than adequate to work with. For instance, the Global Model Quality Estimate (GMQE) of 0.85 showed good coverage of the target sequence and good template structure. Moreover, the QMEANDisCo Global of 0.77 ± 0.05 provided a model with a good local quality score. Both parameters should be taken into account to increase reliability of the quality estimation. It is also important to mention that the RMSD for the alignment process performed in LovoAlign server is 2.15 Å, which can be considered a fair result since AMPK has regions in its subunits that are flexible, and this characteristic can increase the value of the RMSD.[45] The homology model generated by SWISS-Model was validated

using TrRosetta, where the model presented TM-Score greater than 0.5, meaning that the confidence of the model is high.[46] In this way, the structure showed to be reliable to be used in the next steps.

Molecular Docking

In order to predict how the protein would interact with the VC, molecular docking was performed with the conditions previously mentioned in the methodology section. Among the 150 poses generated by the analysis performed, the one that showed lower energy (-103.781 kcal/mol) was chosen for the next step (Figure 5a). In this case, this preferred orientation showed to be more stable than others obtained in this investigation. This study also suggested that the vanadium complex interacts with the following residues: Tyr-205, Thr-211, Pro-213, Leu-212, Asp-215 and Tyr-232 which are highlighted in Figure 5b.

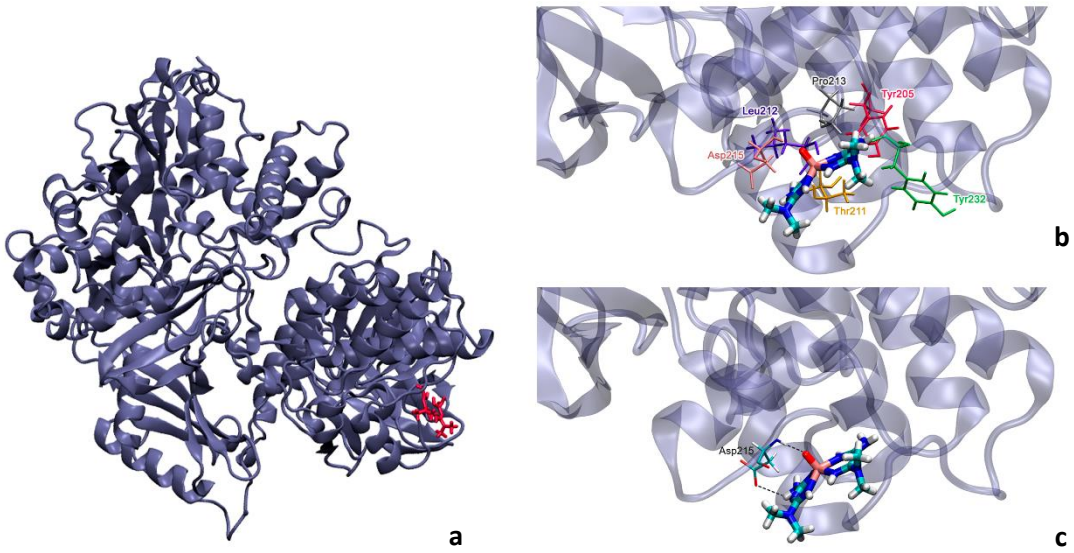

Figure 5. (a) Overview of the system under study. **(b)** Selected pose with lower energy along with residues that interacted with the complex. **(c)** Hydrogen bonds between residue Asp-215 and $VO(metf)_2 \cdot H_2O$.

It is essential to mention that the pose was not elected as a starting point for the simulations solely by its lower energy. As can been seen in Figure 5c, hydrogens bonds between residue Asp-215 and the complex were successfully reproduced in this investigation (Figure 5c). This information of great value **replicated** data already reported in literature.[42] Once information about the orientation and hydrogen bonds made by the

complex was acquired, MD simulations could be initiated, where the system protein-vanadium complex was investigated in a more in-depth way over a period of time.

Molecular Dynamics: application for Alzheimer's treatment

The behavior of the system comprised by AMPK and $VO(metf)_2 \cdot H_2O$ in explicit solvent was monitored during 800 ns and the RMSD was calculated taking as reference the coordinates of the first frame of the simulation. A first look at Figure 6 allows a better comprehension about the VC fluctuations during the time of simulation, where the average RMSD was equal to 0.2578 Å with a standard deviation of 0.0011 Å. The results obtained for the vanadium complex are a great achievement, showing that the molecule remained stable during 800 ns.

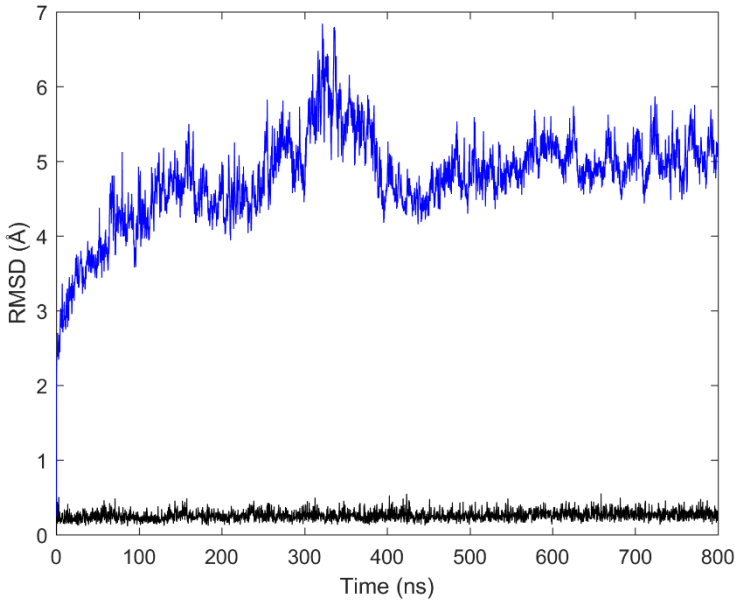

Figure 6. RMSD vs. time graph of the system AMPK-vanadium (IV) complex in explicit solvent. Blue line refers to protein deviation, and black line refers to complex deviation.

The protein, in particular, showed an average RMSD of 4.7774 Å with a standard deviation of 0.0113 Å. These values are quite small considering the reasonable flexibility of its structure.[47]

A sausage representation of the AMPK protein was calculated through software PyMol,[48] where 80 frames were used, 1 frame sampled at every 250 ps of the first 200 ns. As can be seen in Figure 7, the spatial root mean square fluctuation (RMSF) with more displacement are shown in regions with major thickness, i.e., the most mobile regions correspond to major thickness in the sausage representation. Such fluctuations occurred mainly in loop regions, in residues such as Ile-288–Leu-326 (α subunit), Arg-373–Lys-

395 (α subunit), Phe-16–Pro-137 (β subunit), Glu-119–Val-130 (γ subunit), Ala-227–Tyr-241 (γ subunit). This information is consistent with the literature, where it is reported that loops connecting helices and sheets are considered to be more flexible.[49]

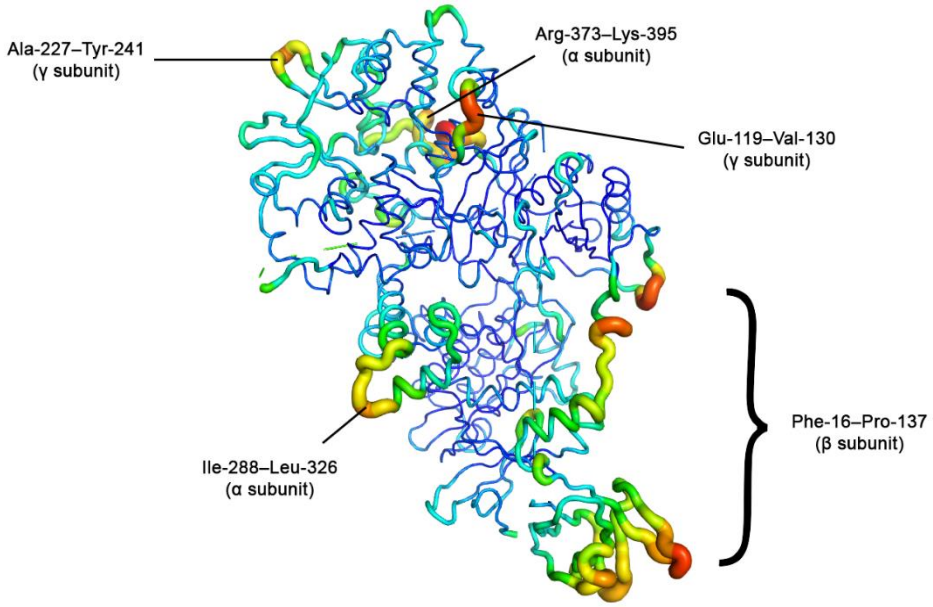

Figure 7. Sausage representation of the superimposed 80 frames of AMPK generated by PyMol v. 2.5.3.

Another aspect of this work that needs to be validated is the hydrogen bonds pointed out during the docking investigation. As stated previously, VO(metf)2·H2O interacted with residues Tyr-205, Thr-211, Pro-213, Leu-212, Asp-215 and Tyr-232.

Based on the information obtained from VMD, taking into account the total time of simulation, it was indicated by the hydrogen bond analysis interactions with residues mentioned on the docking study (Tyr-205, Thr-211, Pro-213, Leu-212, Asp-215 and Tyr-232) in addition to six more residues, namely Tyr-205, Cys-209, Gly-210, Phe-214, Thr-233, and Gln-235.

In particular, interactions between residue Leu-212 and VO(metf)2·H2O were reported as most recurring. Although not reported by the literature, interactions between Leu-212@O and VC@H3, Leu-212@O and VC@I3, and Leu-212@O and VC@I1 were found throughout the simulation, as can be seen in Figure 8.

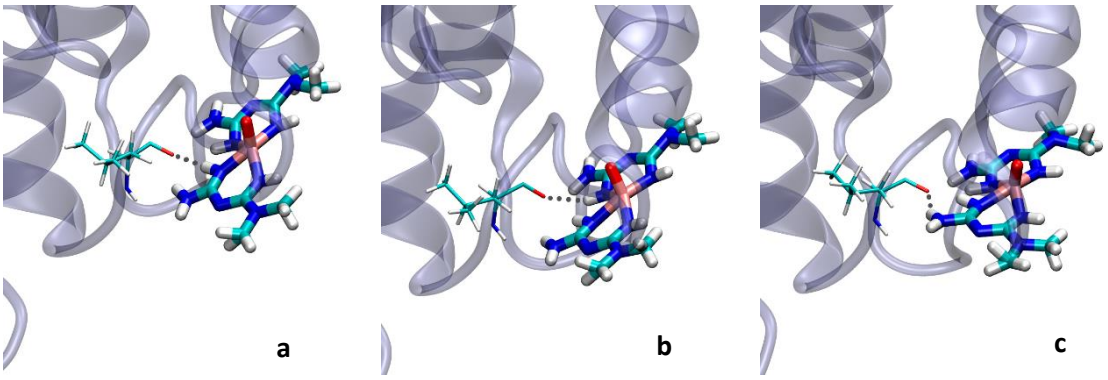

Figure 8. Hydrogen bonds between **(a)** Leu-212@HB2 and VC@N7, **(b)** Leu-212@HB2 and VC@N2 and **(c)** Leu-212@HB2 and VC@N6.

Interestingly, residue Gln-235 participated in the formation of hydrogen bonds as well, and was not pointed out during the docking study, considering the chosen pose. Furthermore, interactions with this residue were the second most recurring. Residue Gln-235@H forms a hydrogen bond with VC@O1. Such interaction was possible due to the displacement of the complex over the last 65 ns of the simulation. This behavior will be addressed next.

Due this displacement, hydrogen bonds between VC and residues Cys-209 and Gly-210 were also reported, where VC@O1 and Cys209@HB3, and VC@H4 interacted Gly210@O were pointed out by the MD. In this case, these interactions were not described by the literature.

Another interaction noteworthy is the hydrogen bonds between Asp-215@H and VC@O1, and between Asp-215@H and VC@N6, that was not described by the literature. In addition, the interaction between nitrogen (N6) from VC and the hydrogen from the same residue were corroborated in this analysis.

Hydrogen bonds formed between residues Tyr-205, Thr-211, Pro-213, Phe-214, Tyr- 232, and Thr-233 and the vanadium complex were also confirmed by this analysis, however the occurrence of such bonding was less significant.

Throughout most of the simulation, the protein did not undergo any drastic change. However, it was observed a change in conformation in residues Leu-208 to Asn-238 in the last 615 ns of the simulation, as can be seen in Figure 9.

This conformation change may have affected interactions between VC and residues, such as Asp-215 and Leu-212, in which may have distanced themselves from $VO(metf)_2 \cdot H_2O$. Presumably, during this conformational change, residues Cys-209,

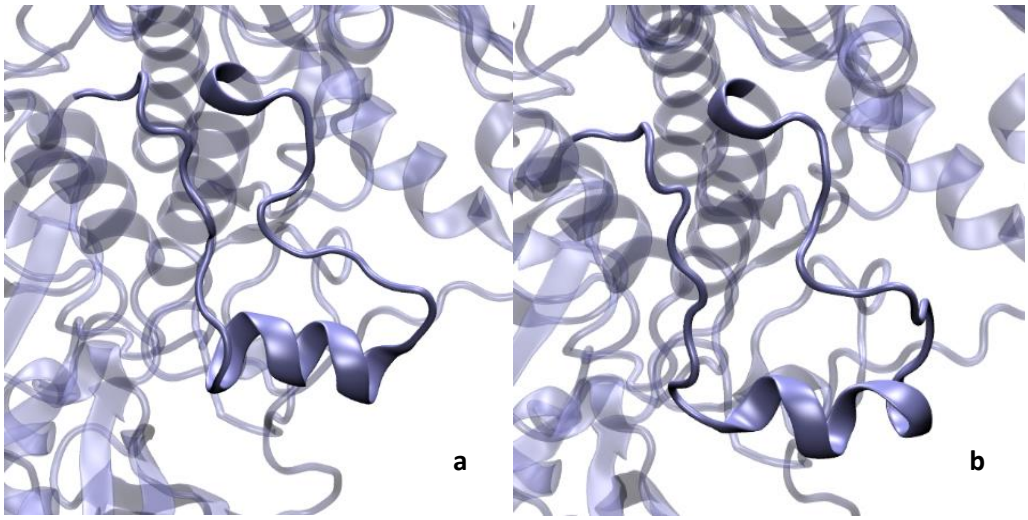

Figure 9. Residues Leu208 to Asn238 undergoing through conformational change. **(a)** Before the change. **(b)** After conformational change.

Gly210, and Gln-235 may have approached VC and then a more effective hydrogen bond between those species was formed.

Furthermore, over the 800 ns of simulation, the loops shown in Figure 9 experienced oscillations that might have contributed to the displacement of the complex and formation of the hydrogen bond with the already mentioned residues. Another change that might have contributed is the α-helix, where its length showed considerable variation due to conformation change.

Taking into consideration the fact that AMPK plays key roles in both T2DM and AD,[9] being considered as a bridge between these two diseases, and the promising effects of VC in facing T2DM, turning into a potential agent against the neurodegenerative disease in question, the encouraging results obtained by this work may offer valuable insights in the AD treatment.

4. Conclusion

The present work aimed to understand in a more refined way the interaction of the VC and the AMPK protein (associated with AD and T2DM). To this end, the work consists of two stages which show the relevance and important contribution of the findings to the scientific community.

The first one was motivated by the lack of structural information of the vanadium complex under study in this work. Through computational tools, an AMBER force field was developed and validated using a strategy that showed to be efficient to describe the VC, $VO(metf)_2 \cdot H_2O$.

The mean relative errors for bond lengths and bond angles proved to be considerably small, reinforcing an acquisition of a great geometry. Supported by RMSD analysis, the proposed specific metal-ligand set of parameters lead to an equilibrium condition and stable conformation. Lastly, BLA analysis showed that the new force field was able to reproduce the experimental prediction. Overall, the new parameter set showed better performance that the general and widely used GAFF.

After encouraging results, the second stage for the investigation was carried out, where the biological application, i.e., the interactions and behavior of the system formed by the protein and $VO(metf)_2 \cdot H_2O$ were the focus of the research. Furthermore, the hydrogen bonds pointed out during docking were validated. It is worth mentioning residue Leu-212 as the residue that interacted most with the complex.

Once again, RMSD analysis provided a better understanding of how the system behaved during the simulation time. RMSD values for the VC were considered excellent for this study, where the complex showed stability during the total time of simulation. In turn, the RMSD values of the protein proved to be in line with expectations since the structure has considerable flexibility. Residues Cys-209, Gly210, Phe-214 and Gln-235 that interacted with the molecule after a conformational change of the protein in a specific region near the binding site should be highlighted as well. In general, the results obtained in this step provide a meaningful insight into the behavior of the system under study.

These findings obtained in this work can be considered motivating for future studies that have the purpose of using the vanadium complex for the treatment of AD, since this molecule in question can be considered promising for this specific application, as mentioned before, where improving interactions between residues such as Leu-212 and Asp-215 and the VC may be an excellent approach.

Supporting Information

Equivalence of residues from original structure and from the model; all structure information associated with the vanadium complex different methods and levels of theory, including bond and angles; comparisons of mean of relative errors; parameter file for vanadium complex; RESP charges for the complex, potential energy surface of dihedrals for different methods; RMSD of VC in aqueous solution.

Supporting Information.docx

Author Contributions

C.A.T. developed the project;

C.A.T., T.C.R. and E.F.F.C. analyzed the data;

C.A.T., T.M.R.S., and T.C.R. wrote the paper;

T.C.R. conceived the overarching project.

Funding Sources

This work is financially supported by the Brazilian agencies CAPES, CNPq, and FAPEMIG.

Notes

The authors declare no conflict of interest.

Acknowledgements

The authors thank Ander Francisco Pereira for the assistance with the methodology and the comments that greatly improved the manuscript.

References

(1) United Nations, Department of Economic and Social Affairs, Population Division (2022). *World Population Prospects 2022*, Online Edition, available at: https://population.un.org/wpp/Download/Standard/Mortality/ [accessed 1 September 2022].

(2) World Health Organization, Newsroom, Fact Sheets, Detail (2022). *Dementia*, Online Edition, available at: https://www.who.int/news-room/fact-sheets/detail/dementia [accessed 1 September 2022]

(3) Volicer, L. Physiological and pathological functions of beta-amyloid in the brain and Alzheimer's disease: A review. *Chin. J. Physiol*. **2020**, 63, 3, 95, 2020.

(4) Falco, A. D.; Cukierman, D. S.; Hauser-Davis, R. A.; Rey, N. A. Doença de Alzheimer: hipóteses etiológicas e perspectivas de tratamento. *Quim. Nova*. **2016**, 39, 63-80.

(5) Paudel, P.; Park, C. H. Jung, H. A.; Yokozawa, T., Choi, J. S. A systematic review on anti-Alzheimer's disease activity of prescription Kangen-karyu. *Drug Discov. Ther*. **2020**, 14, 61-66.

(6) Nguyen, P. H.; Ramamoorthy, A; Sahoo, B. R.; Zheng, J.; Faller, P.; Straub, J. E.; Dominguez, L.; Shea, J. E.; Dokholyan, N. V.; Simone, A. *et al*. Amyloid oligomers: A joint experimental/computational perspective on Alzheimer's disease, Parkinson's disease, type II diabetes, and amyotrophic lateral sclerosis. *Chem. Rev.* **2021**, 121, 4, 2545-2647.

(7) Doig, A. J.; Castillo-Frias, M. P.; Berthoumieu, O.; Tarus, B.; Nasica-Labouze, J.; Sterpone, F.; Nguyen, P. H.; Hooper, N. M.; Faller, P.; Derreumaux, P. Why is research on amyloid-β failing to give new drugs for Alzheimer's disease? *ACS Chem. Neurosci.* **2017**, 8, 7, 1435-1437, 2017.

(8) Bortoletto, A. S.; Graham, W. V.; Trout, G.; Bonito-Oliva, A.; Kazmi, M. A.; Gong, J.; Weyburne, E.; Houser, B. L.; Sakmar, T. P.; Parchem. R. J. Human Islet Amyloid Polypeptide (hIAPP) Protofibril-Specific Antibodies for Detection and Treatment of Type 2 Diabetes. *Adv. Sci*. **2022**, 9, 34, e2202342.

(9) Chen, M.; Huang, N.; Liu, J.; Huang, J.; Shi, J.; Jin, F. AMPK: A bridge between diabetes mellitus and Alzheimer's disease. *Behav. Brain. Res*. **2021**. 400, 113043.

(10) Kang, P.; Wang, Z.; Qiao, D.; Zhang, B.; Mu, C.; Cui, H.; Li, S. Dissecting genetic links between Alzheimer's disease and type 2 diabetes mellitus in a systems biology way. *Front. Genet*. **2022,** 13.

(11) Peixoto, C. A.; Oliveira, W. H.; Araújo, S. M. R.; Nunes, A. K. S. AMPK activation: Role in the signaling pathways of neuroinflammation and neurodegeneration. *Exp. Neurol*. **2017,** 298, 31-41.

(12) Ge, Y.; Zhou, M.; Chen, C.; Wu, X.; Wang, X. Role of AMPK mediated pathways in autophagy and aging. *Biochimie*. **2022**, 195, 100-113.

(13) Andrade, C. H.; Kummerle, A. E.; Guido, R. V. C. Perspectivas da química medicinal para o século XXI: desafios e oportunidades. *Quim. Nova*. **2018,** 41, 476-483.

(14) Akter, K.; Lanza, E. A.; Martin, S. A.; Myronyuk, N.; Rua, M.; Raffa. R. B. Diabetes mellitus and Alzheimer's disease: shared pathology and treatment? *Br. J. Clin. Pharmacol*. **2011**, 71, 3, 365-76.

(15) Liu, H.; Qu, Y.; Wang, X. Amyloid β-targeted metal complexes for potential applications in Alzheimer's disease. *Future Med. Chem*. **2018**, 10(6), 679-701.

(16) Rusanov, D. A.; Zou, J.; Babak, M. V. Biological Properties of Transition Metal Complexes with Metformin and Its Analogues. *Pharmaceuticals*. **2022**, 15, 4.

(17) Woo, L. C. Y.; Yuen, V. G.; Thompson, K. H.; McNeill, J. H.; Orvig, C. Vanadyl–biguanide complexes as potential synergistic insulin mimics. *J. Inorg. Biochem*. **1999**, 76, 3, 251-257.

(18) Karplus, M.; McCammon, J. A. Molecular dynamics simulations of biomolecules. Nat. Struct. Biol. **2002**, 9, 9, 646-652.

(19) Salo-Ahen, O. M. H.; Alanko, I.; Bhadane, R.; Bonvin, A. M. J. J.; Honorato, R. V.; Hossain, S.; Juffer, A. H.; Kabedev, A.; Lahtela-Kakkonen, M.; Larsen, A. S. *et al*. Molecular dynamics simulations in drug discovery and pharmaceutical development. *Process*. **2020**, 9, 1, 71.

(20) Li, P.; Merz Jr, K. M. Metal Ion Modeling Using Classical Mechanics. *Chem. Rev*. **2017**, 117, 3, 1564-1686.

(21) Pereira, A. F.; Prandi, I. G.; Ramalho, T. C. Parameterization and validation of a new force field for Pt(II) complexes of 2-(4′-amino-2′-hydroxyphenyl)benzothiazole. *Int. J. Quantum Chem*. **2021**, 121, 6, e26525.

(22) Prandi, I. G.; Viani, L.; Andreussi, O.; Mennucci, B. Combining classical molecular dynamics and quantum mechanical methods for the description of electronic excitations: The case of carotenoids. *J. Comput. Chem*. **2016**, 37, 11, 981-991.

(23) Dennington, J. M.; Keith, R. D.; Millam, T. A. *GaussView 5.0.8*, Gaussian. Inc., Wallingford CT. **2008**.

(24) Grimme, S. Semiempirical GGA-type density functional constructed with a long-range dispersion correction. *J. Comput. Chem*. **2006**, 27, 15, 1787-1799.

(25) Frisch, M. J; Trucks, G. W.; Schlegel, H. B.; Scuseria, G. E.; Robb, M. A.; Cheeseman, J. R; Scalmani, G.; Barone, V.; Petersson,G. A.; Nakatsuji, H. *et al*. *Gaussian 16, Revision C.01*, Gaussian. Inc., Wallingford CT, **2016**.

(26) Kaur, N.; Kumari, I.; Gupta, S; Goel, N. Spin Inversion Phenomenon and Two-State Reactivity Mechanism for Direct Benzene Hydroxylation by V4O10 Cluster. *J. Phys. Chem A*. **2016**, 120, 48, 9588-9597.

(27) *HyperChem Professional 7.0*, Hypercube, Inc., Gainesville FL, **2002**.

(28) Neese, F., Software update: the ORCA program system, version 4.0. WIREs Comput. Mol. Sci. **2018**, 8, 1, e1327.

(29) Cárdenas, G.; Marquetand, P.; Mai, S.; González, L. A Force Field for a Manganese-Vanadium Water Oxidation Catalyst: Redox Potentials in Solution as Showcase. *Catalysts*. **2021**, 11, 4.

(30) Santos, L. A.; Prandi, I. G.; Ramalho, T. C. Could Quantum Mechanical Properties Be Reflected on Classical Molecular Dynamics? The Case of Halogenated Organic Compounds of Biological Interest. Front. Chem. **2019**, 7.

(31) Humphrey, W.; Dalke, A.; Schulten, K. VMD: Visual molecular dynamics. *J. Mol. Graph.* **1996**, 14, 1, 33-38.

(32) Cornell, W. D.; Cieplak, P.; Bayly, C. I.; Gould, I. R.; Merz Jr, K. M.; Ferguson, D. M.; Spellmeyer, D. C.; Fox, T.; Caldwell, J. W.; Kollman, P. A. A Second Generation Force Field for the Simulation of Proteins, Nucleic Acids, and Organic Molecules. *J. Am. Chem. Soc*. **1995**, 117, 19, 5179-5197.

(33) Monticelli, L.; Tieleman, D.P. Force Fields for Classical Molecular Dynamics. In *Biomolecular Simulations: Methods and Protocols*, Humana Press, **2013**; pp. 197-213.

(34) Zheng, S.; Tang, Q.; He, J.; Du, S.; Xu, S.; Wang, C.; Xu, Y.; Lin, F. VFFDT: A New Software for Preparing AMBER Force Field Parameters for Metal-Containing Molecular Systems. *J. Chem. Inf. Model*. **2016**, 56, 4, 811-818.

(35) Šebesta, F., Sláma, V.; Melcr, J.; Futera, Z.; Burda, J. V. Estimation of Transition-Metal Empirical Parameters for Molecular Mechanical Force Fields. *J. Chem. Theory Comput.* **2016**, 12, 8, 3681-3688.

(36) Case, D. A.; Darden, T. A.; Cheatham, T. E.; III, Simmerling, C. L.; Wang, J.; Duke, R. E.; Luo, R.; Walker, R. C.; Zhang, W.; Merz, K. M. *et al*. *AMBER 11*, University of California, San Francisco CA, **2010**.

(37) Yan, Y.; Zhou, E.; Novick, S. J.; Shaw, S. J.; Li, Y.; Brunzelle, J. S.; Hitosh, Y.; Griffin, P. R.; Xu, H. E. Melcher, K. Structures of AMP-activated protein kinase bound to novel pharmacological activators in phosphorylated, non-phosphorylated, and nucleotide-free states. J. Biol. Chem. **2019**, 294, 3, 953-967.

(38) Waterhouse, A.; Bertoni, M.; Bienert, S.; Studer, G.; Tauriello, G.; Gumienny, R.; Heer, F. T.; Beer, T. A. P.; Rempfer, C.; Bordoli, L. *et al*. SWISS-MODEL: homology modelling of protein structures and complexes. *Nucleic Acids Res*. **2018**, 46, W1, W296-W303.

(39) Martínez, L.; Andreani, R.; Martínez, J.M. Convergent algorithms for protein structural alignment. *BMC Bioinform*. **2007**, 8, 1, 306.

(40) *BIOVIA Discovery Studio Visualizer*. Dassault Systèmes, San Diego CA, **2021**.

(41) *Molegro Virtual Docker*. Molexus, Rørth Denmark, **2011**.

(42) Thabah, D.; Syiem, D.; Pakyntein, C.; Banerjee, S.; Kharshiing, C. E.; Bhattacharjee, A. Potentilla fulgens upregulate GLUT4, AMPK, AKT and insulin in alloxan-induced diabetic mice: an in vivo and in silico study. Arch. Physiol. Biochem. **2021**, 1-13.

(43) Thomsen, R.; Christensen, M.H. MolDock: A New Technique for High-Accuracy Molecular Docking. *J. Med. Chem*. **2006**, 49, 11, 3315-3321.

(44) Aledavoo, E.; Forte, A.; Estarellas, C.; Luque, J. Structural basis of the selective activation of enzyme isoforms: Allosteric response to activators of β1- and β2-containing AMPK complexes. *Comput. Struc. Biotechnol. J*. **2021**, 19, 3394-3406.

(45) Martínez, L. Automatic Identification of Mobile and Rigid Substructures in Molecular Dynamics Simulations and Fractional Structural Fluctuation Analysis. PLoS ONE. **2015**, 10, 3, e0119264.

(46) Du, Z.; Su, H.; Wang, W.; Ye, L.; Wei, H.; Peng, Z.; Anishchenko, I.; Baker, D.; Yang, J. The trRosetta server for fast and accurate protein structure prediction. *Nat. Protoc*. **2021**, 16, 12, 5634-5651.

(47) Kurumbail, R.G. and M.F. Calabrese, Structure and Regulation of AMPK. In *AMP-activated Protein Kinase*, Springer, **2016**; pp. 3-22.

(48) *The PyMOL Molecular Graphics System*. Schrödinger, LLC, **2015**.

(49) Subramani, A. Floudas, C.A. Structure prediction of loops with fixed and flexible stems. *J. Phys. Chem. B.* **2012**, 116, 23, 6670-6682.

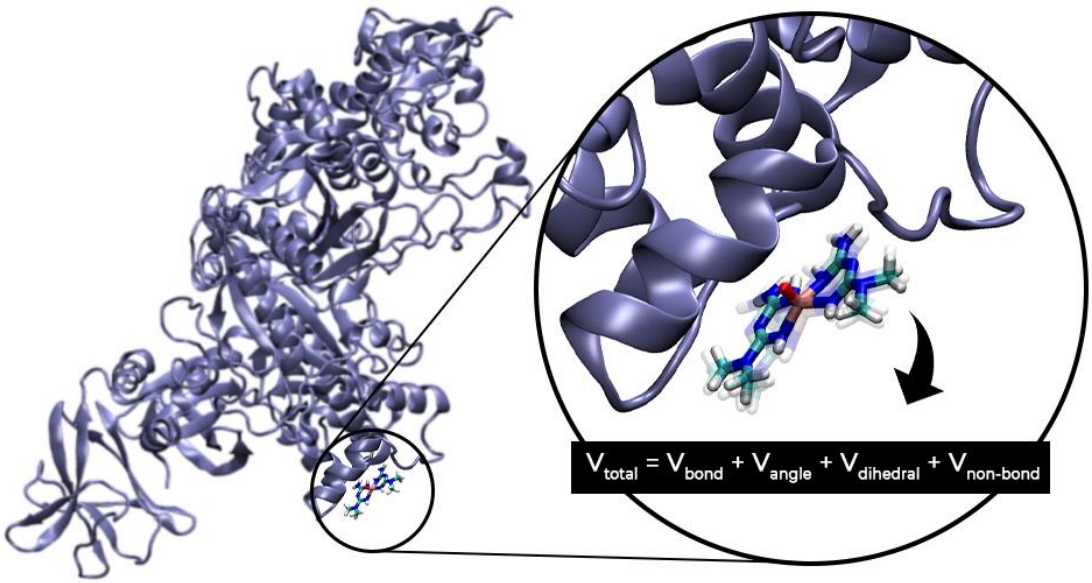
$V_{total} = V_{bond} + V_{angle} + V_{dihedral} + V_{non\text{-}bond}$